Space-time localized structures in the degenerate optical parametric oscillator

M. Tlidi and Paul Mandel

Optique Nonlinéaire Théorique, Campus Plaine Code Postal 231, Université Libre de Bruxelles, 1050 Bruxelles, Belgium

(Received 2 September 1998)

We study the transverse effects in a degenerate optical parametric oscillator with a saturable absorber. We focus on the analysis of two-dimensional stationary and time-dependent localized patterns. The homogeneous steady-state solution is destabilized by a Hopf bifurcation to periodic states with finite wave number and a Turing bifurcation. These bifurcations are close enough that they interact. This leads to localized structures consisting of a sharp peak emitting concentric rings of alternating high and low intensities.
[S1050-2947(99)50204-7]

PACS number(s): 42.65.Sf, 42.65.Pc, 42.60.Mi

Stationary localized structures (also called spatial solitons) associated with homoclinic connections between coexisting stable steady states are now attracting growing interest in optics because of their potential application in information technology. Such localized structures (LS) have been predicted in an early report on bistable systems [1]. Later, it was shown that the existence of LS does not require a bistable homogeneous steady state. They can be stable in the monostable regime [2] where the single homogeneous steady state exhibits a subcritical Turing (or modulational) instability leading to a pattern forming process characterized by an intrinsic wavelength that is determined by dynamical parameters and not by geometrical constraints imposed by the cavity boundaries or system's physical dimensions. Stationary LS have been also obtained in a Kerr medium [3,4], a purely dispersive two-level medium [5], a quadratic medium [6,7], semiconductor devices [8], and a spin-1/2 atomic system [9]. The LS can exhibit chaotic oscillations in time [10]. Recently, the experimental evidence for LS in optical systems [11] has further stimulated the interest in the transverse pattern formation process.

Up to now, investigations on two-dimensional (2D) LS in optics have been limited to situations where the homogeneous background is stable against oscillatory modes. The purpose of this paper is to study the dynamics of LS in a situation where Turing and Hopf bifurcations interact. In this regime, stationary and/or time-dependent LS appear. We report evidence of LS that consists of a 2D stationary peak in the transverse profile of the cavity field. In the time-dependent regime, these peaks emit traveling waves forming concentric rings. The amplitude of the central peaks is essentially the same as the corresponding static Turing structures. These solutions have already been described in one transverse dimension [7].

We consider a ring cavity, driven by a coherent plane wave, filled by a nonlinear medium in which frequency conversion takes place. We focus on degenerate intracavity optical parametric amplification: one photon with frequency 2ω is absorbed and two photons with frequencies ω are emitted. In addition, we assume the presence of a saturable absorber that absorbs the field at frequency ω. The effective absorption coefficient is therefore field dependent and is modeled by a saturable two-level medium. This model for the degenerate optical parametric oscillator with a saturable absorber (DOPOSA) was introduced in Ref. [12]. Assuming fast atomic relaxation and the mean-field approximation, the evolution equations in reduced variables are

$$\frac{\partial E_1}{\partial t} = -E_1 + E_1^* E_2 - \frac{RE_1}{1+S|E_1|^2} + ia_1 \mathcal{L}_\perp E_1, \qquad (1)$$

$$\frac{\partial E_2}{\partial t} = -\gamma(E_2 + E_1^2 - E_i) + ia_2 \mathcal{L}_\perp E_2. \qquad (2)$$

$E_{1,2}$ are the normalized slowly varying envelopes of the signal and the pump fields at frequencies ω and 2ω, respectively. E_i is the driving field that is chosen real to fix the reference phase. γ is the ratio of the photon lifetimes at frequencies ω and 2ω. The saturable absorber is characterized by its saturation intensity $1/S$ and its linear loss coefficient R, a_1 and a_2 are the diffraction coefficients, and $\mathcal{L}_\perp = \partial^2/\partial x^2 + \partial^2/\partial y^2$ is the Laplace operator acting on the transverse plane (x,y). The phase-matching condition imposes that $a_1/a_2 = 2$ [13]. Time has been scaled such that the decay rate of mode 1 is unity. Space is scaled in such a way that $a_1 = 1$ and $a_2 = 1/2$.

Equations (1) and (2) admit two types of homogeneous steady-state solutions: (i) the nonlasing state $\overline{E_1} = 0$ and $\overline{E_2} = E_i$ that is stable below the lasing threshold $E_i < E_{th} = 1 + R$; (ii) the lasing state $E_i = 1 + \overline{I_1} + R/(1 + S\overline{I_1})$ and $\overline{E_2} = E_i - \overline{E_1^2}$. The steady state $\overline{I_1} = |\overline{E_1}|^2$ as a monotonic function of E_i if $RS < 1$; it is bistable if $RS > 1$. The linear stability of these solutions with respect to perturbations of the form $\exp(\lambda t + i\mathbf{k}\cdot\mathbf{r})$ where $(\mathcal{L}_\perp + k^2)\exp(\lambda t + i\mathbf{k}\cdot\mathbf{r}) = 0$ has been studied in Ref. [7].

The homogeneous lasing steady-state solution can be destabilized by the competition between two processes: diffraction that tends to restore spatial uniformity in the transverse plane and the nonlinearities (quadratic medium and saturable absorber) that are responsible for the amplification of the spatial inhomogeneities. The balance between the two processes generates a well known Turing (or modulational) instability [14] leading to the formation of intrinsic stationary periodic patterns characterized by the wavelength $\Lambda_T = 2\pi/k_T$ where

$$k_T^4=\gamma(\overline{I}_{1T}-\gamma/2)-\frac{RS\overline{I}_{1T}(1+R+S\overline{I}_{1T})}{2(1+S\overline{I}_{1T})^3},$$

and I_{1T} is the critical intensity at the Turing bifurcation. It is the solution of

$$(2\overline{I}_{1T}+\gamma)(\beta_{-T}^2-\beta_{+T}^2+4\gamma^2)=2\gamma(4\beta_{-T}\overline{I}_{1T}+3\gamma^2), \tag{3}$$

where $\beta_{\pm}=\pm1\pm\alpha R(1\pm\alpha S\overline{I}_1)$ and $\beta_{\pm T}$ is evaluated at $\overline{I}_1=\overline{I}_{1T}$. The lasing steady state undergoes a Hopf bifurcation if a pair of complex-conjugate eigenvalues has a vanishing real part with a finite imaginary part. This instability occurs at $\overline{I}_1=\overline{I}_{1H}$, which is the solution of

$$b(\overline{I}_{1H},k)[2(\gamma-\beta_-)-b(\overline{I}_{1H},k)]=4(\gamma-\beta_-)a(\overline{I}_{1H},k) \tag{4}$$

with $b(\overline{I}_1,k)=2\gamma(\beta_-^2-\beta_+^2)+4\gamma\overline{I}_1(\gamma-\beta_-)-2\beta_-(\gamma^2+k^4)+8\gamma k^4$, $a(\overline{I}_1,k)=(\beta_-^2-\beta_+^2+4k^4)(\gamma^2+k^4)-4\gamma\overline{I}_1(\gamma\beta_-+2k^4-\gamma\overline{I}_1)$, and $\alpha=1/(1+S\overline{I}_1)$. The frequency of the periodic solution at the Hopf bifurcation is

$$\Omega(\overline{I}_{1H},k)=\sqrt{b(\overline{I}_{1H},k)/2}. \tag{5}$$

The homogeneous time-periodic mode has maximum gain. The threshold associated with this instability, obtained by solving Eq. (4) with $k=0$, is $\overline{I}_{1H\pm}(k=0)\equiv J_{1H\pm}=(R-\gamma\pm\sqrt{R(R-2\gamma)}/(\gamma S)$ with critical frequency $\Omega_H=\Omega(J_{1H\pm},0)=\sqrt{\gamma(2J_{1H\pm}-\gamma)}$. The Hopf instability with $k\neq0$ always arises for $I_1>I_{1H-}$. We fix $\gamma=1$, $S=0.1$ and let R and E_i be the control parameters. For these parameters, there are two pairs of Hopf and Turing instabilities. We focus on the pair of Hopf and Turing bifurcations that occur first when the input field amplitude is increased. The relative order between the two bifurcations is controlled by the linear loss of the saturable absorber. If $R<R_c\approx5.47$ the Hopf bifurcation occurs before the Turing instability.

In the vicinity of the codimension-two-point $R=R_c$ where the two bifurcations coalesce, a weakly nonlinear analysis of Eqs. (1) and (2) has shown that the system can exhibit bistable behavior not only between the homogeneous steady state and the Turing branch but also between the static Turing and the homogeneous Hopf branches [7]. In addition, when the static Turing branch becomes unstable, a stable solution emerges from the homogeneous steady state, the so-called mixed-mode solution corresponding to periodic oscillation in time and space. A completely different mechanism for the generation of mixed-mode solutions is a Hopf bifurcation located at the Turing branch. This secondary bifurcation arises as a result of a nonlinear interaction between transverse unstable modes. This behavior was described in the case of two counterpropagating coherent beams in a Kerr medium [15] and in the Lugiato-Lefever model [3,16]. Intracavity second-harmonic generation, neglecting diffraction but including chromatic dispersion, leads to either Turing or Hopf bifurcations [17]. An analytical stability analysis of this model shows that the homogeneous Hopf and Turing branches lose their stability in favor of a mixed-mode branch that is stable over a large range of parameters [18].

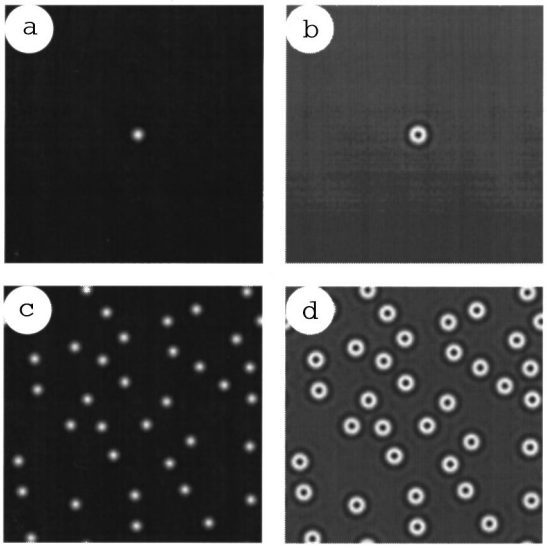

FIG. 1. 2D localized structures. Parameters are $\gamma=1$, $R=4.5$, $S=0.1$, and $E_i=5.75$. Single localized structure obtained after perturbing the stable homogeneous steady state at one grid point, the amplitude of the perturbation $\Delta|E_1|=10$ and $\Delta|E_2|=2$. (a) Real part of the signal field E_1; (b) real part of the pump field E_2. Random distribution of localized structures obtained from a small-amplitude random noise initially added to $|E_1|=15$ and $|E_2|=5$. (c) real part of the signal field E_1; (d) real part of the pump field E_2. Maxima are plain white and mesh number integration is 128×128.

To analyze the implications of the interaction between the Hopf and the Turing bifurcations in the dynamics of the 2D LS, we select parameters leading to the monostable homogeneous steady state and fix $R=4.5$. The critical Hopf bifurcation ($E_i=E_H$) occurs in the hysteresis domain involving the homogeneous steady state and the hexagonal structures. Note that for $R=4.5$ stripes are not observed. Let us consider first the domain of input field where the hexagonal structures and the homogeneous steady state are stable for the same value of the input field. This occurs before the Hopf bifurcation ($E_i<E_H$). In this domain 2D stationary stable localized structures can be generated, an example of which is displayed in Fig. 1(a) where we plot the transverse profile of $\mathrm{Re}(E_1)$. The boundary conditions used in all our numerical simulations are periodic. These LS connect the homogeneous steady state to the hexagonal state. The number and the position of the stationary peaks depend on the initial conditions. They are stable against small variations of their positions. The LS can also be randomly distributed in the transverse plane [see Figs. 1(c) and 1(d)]. They are thus of the same nature as the LS analyzed in our previous work [2]. However, for the pump field E_2, the 2D transverse profile is characterized by rings encircling a dip [see Figs. 1(b) and 1(d)]. This behavior is explained by the fact that signal and the pump fields are out of phase. To stabilize the LS, the pump field must have a minimum amplitude where the signal field amplitude has a maximum.

As the input field is increased beyond the Hopf bifurcation, the LS become time dependent. They are characterized by a stationary strongly localized peak for both E_1 and E_2.

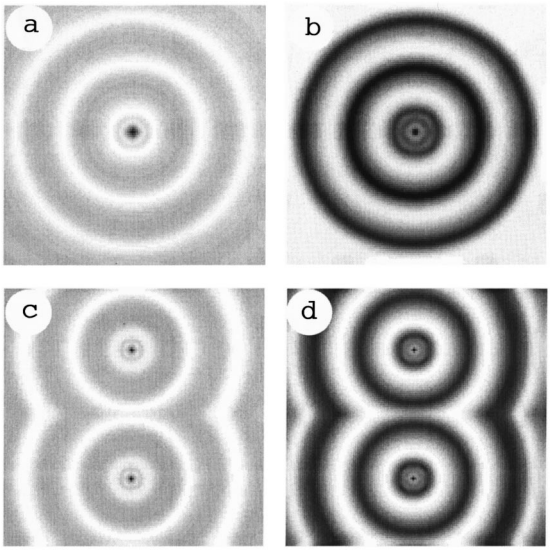

FIG. 2. 2D time-dependent localized structures. Parameters are $\gamma=1$, $R=4.5$, $S=0.1$, and $E_i=6.5$. The initial condition is the profile obtained in Figs. 1(a) and 1(b). Isolated localized structure: (a) real part of the signal field; (b) real part of the pump field. Two localized structures: (c) real part of the signal field; (d) real part of the pump field. Maxima are plain white and mesh number integration is 128×128.

In Figs. 2(a) and 2(b) we show a single LS, while in Figs. 2(c) and 2(d) we display two interacting LS. The number of LS and their positions depend only on the initial condition, and their amplitudes are essentially the same as the coexisting hexagonal structure. The prominent feature is that each peak emits concentric waves. To analyze this behavior, we make a cross section at the center of Figs. 2(a) and 2(b), parallel to the y direction, for the signal and pump fields. This section is shown in Fig. 3. This self-organized spatiotemporal behavior originates from the amplification of

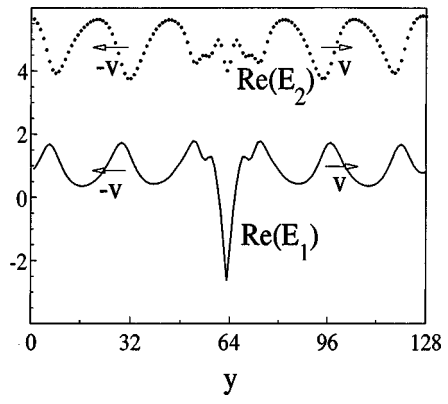

FIG. 3. Cross section taken from Figs. 2(a) and 2(b) passing through the center of the transverse plane. The labeling of the y axis is the number of mesh points. The increment between two consecutive points is 0.8 so that the dimensionless transverse length is 102.4.

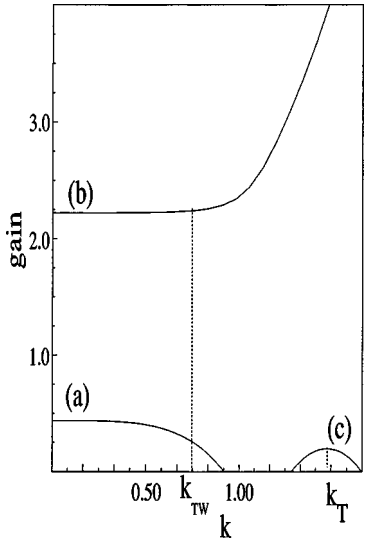

FIG. 4. Gain versus the transverse wave number for $\gamma=1$, $R=4.5$, $S=0.1$, and $\overline{I_1}=2.8$. (a) and (b) are, respectively, the real and the imaginary parts of the eigenvalues λ obtained from the linear stability analysis. (c) is the stability curve associated with the Turing instability.

time-dependent modes with nonzero wave vectors. As we have seen from the above linear stability analysis, there exists a Hopf bifurcation with finite wave number that always appears for E_i larger than the threshold associated with the homogeneous Hopf bifurcation. This instability leads to the formation of traveling waves (TW) that are emitted in phase to the left and to the right of the peaks located at the center of transverse space (see Fig. 3). The wave number k_{TW}, which characterizes the TW solutions, is exactly half the most unstable mode associated with the static Turing instability $k_{TW}=k_T/2$ (see Fig. 4). This means that the wavelength of the TW solutions is twice as large as the coexisting hexagonal stationary structure $\lambda_{TW}=2\lambda_T$. The velocity of the TW emitted from the center is $|v|=\Omega(k_{TW})\lambda_{TW}/2\pi$. The value of the inhomogeneous Hopf frequency $\Omega(k_{TW})$ can be calculated from Eq. (5). It is found to be close to the homogeneous Hopf frequency. In fact, as shown in Fig. 4 [curve (b)], the imaginary part of the root is practically constant: $\Omega(k_{TW})\approx\Omega_H$ for $k<1$.

To summarize, we have shown that LS can be generated on an oscillatory background by studying a degenerate optical parametric oscillator for a range of parameters where Hopf and Turing bifurcations interact. The steady LS found below the Hopf bifurcation are characterized by a sharp maximum and out-of-phase fields (peak for E_1 and dip for E_2). In the vicinity of the Hopf bifurcation, the LS change dramatically. The LS associated with both fields display a central peak surrounded by rings generated by traveling waves emanating from the peak.

This research was supported in part by the Fonds National de la Recherche Scientifique (Belgium) and the Inter-University Attraction Pole program of the Belgian government.

[1] N. N. Rosanov and G. V. Khodova, Opt. Spectrosk. **72**, 1394 (1992) [Opt. Spectrosc. **72**, 782 (1992)]; N. N. Rosanov, Proc. SPIE **1840**, 130 (1992).

[2] M. Tlidi, P. Mandel, and R. Lefever, Phys. Rev. Lett. **73**, 640 (1994); M. Tlidi and P. Mandel, Chaos Solitons Fractals **4**, 1457 (1994).

[3] A. J. Scroggie, W. J. Firth, G. S. McDonald, M. Tlidi, R. Lefever, and L. A. Lugiato, Chaos Solitons Fractals **4**, 1323 (1994).

[4] W. J. Firth and A. Lord, J. Mod. Opt. **43**, 1071 (1996).

[5] W. J. Firth and A. J. Scroggie, Phys. Rev. Lett. **76**, 1623 (1996); M. Brambilla, L. A. Lugiato, and M. Stefani, Europhys. Lett. **34**, 109 (1996).

[6] S. Longhi, Opt. Lett. **20**, 695 (1995); K. Staliunas and V. J. Sanchez-Morcillo, Opt. Commun. **139**, 306 (1996); S. Longhi, Phys. Scr. **56**, 611 (1997); C. Etrich, U. Peschel, and F. Lederer, Phys. Rev. Lett. **79**, 2454 (1997); S. Longhi, Opt. Lett. **23**, 346 (1998).

[7] M. Tlidi, P. Mandel, and M. Haelterman, Phys. Rev. E **56**, 6524 (1997).

[8] M. Brambilla, L. A. Lugiato, F. Prati, L. Spinelli, and W. J. Firth, Phys. Rev. Lett. **79**, 2454 (1997); L. Spinelli, G. Tissoni, M. Brambilla, F. Prati, and L. A. Lugiato, Phys. Rev. A **58**, 2542 (1998).

[9] Yu. A. Logvin and T. Ackemann, Phys. Rev. E **58**, 1654 (1998).

[10] M. Le Berre, S. Patrascu, E. Ressayre, and A. Tallet, Phys. Rev. A **56**, 3150 (1997).

[11] W. B. Taranenko, K. Staliunas, and C. O. Weiss, Phys. Rev. A **56**, 1582 (1997).

[12] R.-D. Li, P. Mandel, and T. Erneux, J. Opt. Soc. Am. A **8**, 1835 (1991); P. Mandel, *Theoretical Problems in Cavity Nonlinear Optics* (Cambridge University Press, Cambridge, England, 1997).

[13] A. Yariv and P. Yeh, *Optical Waves in Crystals* (Wiley, New York, 1984).

[14] L. A. Lugiato and R. Lefever, Phys. Rev. Lett. **58**, 2209 (1987); G. L. Oppo, M. Brambilla, and L. A. Lugiato, Phys. Rev. A **49**, 2028 (1994).

[15] J. B. Geddes, J. Lega, J. V. Moloney, R. A. Indik, E. M. Wright, and W. J. Firth, Chaos Solitons Fractals **4**, 1261 (1994).

[16] M. Haelterman, S. Trillo, and S. Wabnitz, Opt. Commun. **93**, 343 (1993).

[17] S. Trillo and M. Haelterman, Opt. Lett. **21**, 1114 (1996).

[18] M. Tlidi and M. Haelterman, Phys. Lett. A **239**, 59 (1998).